

LLM-QBench: A Benchmark Towards the Best Practice for Post-training Quantization of Large Language Models

Ruihao Gong^{*1,2} Yang Yong^{*2} Shiqiao Gu^{*2} Yushi Huang^{*1,2} Yunchen Zhang²
Xianglong Liu^{†1} Dacheng Tao³

¹Beihang University ²SenseTime Research ³Nanyang Technological University
{gongruihao, yongyang, gushiqiao, huangyushi}@sensetime.com xlliu@buaa.edu.cn
dacheng.tao@ntu.edu.sg

Abstract

Recent advancements in large language models (LLMs) are propelling us toward artificial general intelligence, thanks to their remarkable emergent abilities and reasoning capabilities. However, the substantial computational and memory requirements of LLMs limit their widespread adoption. Quantization, a key compression technique, offers a viable solution to mitigate these demands by compressing and accelerating LLMs, albeit with potential risks to model accuracy. Numerous studies have aimed to minimize the accuracy loss associated with quantization. However, the quantization configurations in these studies vary and may not be optimized for hardware compatibility. In this paper, we focus on identifying the most effective practices for quantizing LLMs, with the goal of balancing performance with computational efficiency. For a fair analysis, we develop a quantization toolkit LLMC, and design four crucial principles considering the inference efficiency, quantized accuracy, calibration cost, and modularization. By benchmarking on various models and datasets with over 500 experiments, three takeaways corresponding to calibration data, quantization algorithm, and quantization schemes are derived. Finally, a best practice of LLM PTQ pipeline is constructed. All the benchmark results and the toolkit can be found at <https://github.com/ModelTC/llmc>.

1 Introduction

Recently, large Language models (LLMs) such as GPT-4 (OpenAI et al., 2024) have demonstrated unprecedented generative capabilities in the field of natural language processing (NLP), and achieving widespread applications across various industries. However, their substantial computational and storage costs have impeded their further popularization among users. For instance, BLOOM (Touvron et al., 2023), an open-access multilingual LLM with 176 billion parameters, requires a minimum of 350 GB of space merely to store model weights in full-precision (FP16) format. At a minimum, it requires 5×80GB A100 or 9×40GB A800 NVIDIA GPUs to perform inference with this model. Therefore, reducing their serving cost is paramount to further enhance the application of LLMs.

For the aforementioned challenge, model quantization (Nagel et al., 2021) can be an effective resolution strategy. It maps weights and/or activations to a lower-bit data format to reduce memory footprints and accelerate model inference. Existing quantization approaches can be categorized into two types: quantization-aware-training (QAT) (Bhargat et al., 2020; Gong et al., 2019; Esser et al., 2020; Egiazarian et al., 2024; van Baalen et al., 2024) and post-training quantization (PTQ) (Wei et al., 2023a; Jhunjhunwala et al., 2021; Li et al., 2021). Although with prominent high performance, the necessity for QAT to undergo finetuning or retraining with substantial training data and training cost renders it unattainable for the majority of users. Correspondingly, PTQ compresses models without retraining, making

^{*}Equal contribution.

[†]Corresponding authors.

it a preferred method for LLMs due to its minimal resource requirements. Therefore, considering the quantization cost, we do not mention some QAT methods (Du et al., 2024; Liu et al., 2024; 2023) in our paper. On the other hand, quantization can also be classified into non-uniform (Kim et al., 2024; Egiazarian et al., 2024) and uniform quantization. We only benchmark the latter one, since non-uniform quantization needs complex specialized kernels. However, they always slow down inference speed. Besides these, we also notice some approaches (Chee et al., 2024; Tseng et al., 2024) with additional non-negligible computational overhead during inference. Despite their decent performance, we still ignore them in our research due to their unfriendliness towards inference.

Current uniform PTQ methods always evaluate across distinct datasets in different quantization configurations and with simulated quantization. This current state would lead to users being unable to accurately assess the configurations that should be selected for the efficient and accurate quantization of LLMs. To provide a comprehensive quantization options menu for users to obtain hardware-friendly quantized LLMs with high performance, we make a fair benchmark, which considers two aspects: factors influencing LLM quantization and inference efficiency under our design principles. The former perspective encompassed three dimensions, *e.g.*, calibration data, algorithm, and target bits. Consequently, we evaluate across various kinds of tasks and find our best practice, encapsulated within an end-to-end pipeline that realizes both high efficiency and accuracy LLM quantization. This best practice has been integrated into our quantization toolkit, LLMC. Notably, LLMC, a user-friendly, plug-and-play quantization tool, incorporates dozens of outstanding PTQ algorithms, provides the freedom to select quantization strategies, and also supports deploying quantized LLMs on different inference backends (TensorRT-LLM (Nvidia, 2023), PPL-LLM (OpenPPL, 2023), LightLLM (ModelTC, 2023)) and hardware (Nvidia GPU, Qualcomm mobile chips, TPU). In a word, our main contributions can be described as follows:

1. We release a quantization toolkit LLMC supporting dozens of algorithms, models and hardware. LLMC enables users to perform lossless quantization on 100-billion-parameter LLMs within a matter of hours, utilizing just a single GPU. It notably facilitate the research and production of quantized LLMs.
2. We modularly and fairly benchmark the quantization techniques considering calibration cost, inference efficiency, quantized accuracy. Near 600 experiments on diverse models and datasets provide three insightful takeaways on the calibration data, algorithm pipeline and quantization configuration selection.
3. Based on the takeaways, a best practice of LLM PTQ pipeline is designed, achieving the best accuracy and efficiency performance balance under various scenarios.

2 Benchmark Overview

In this section, we first provide our benchmark’s design principles subsection 2.1, outlining its primary objective. We then detail LLM quantization subsection 2.2. In Section. subsection 2.2, after introducing the preliminary of quantization, we overview our exploration in the benchmark, *e.g.*, factors influencing LLM quantization and inference efficiency. Finally, we exhibit our plug-and-play quantization toolkit within our benchmark.

2.1 Design Principles

Our benchmark focuses on four essential aspects for effective and practical LLM quantization: inference performance, calibration cost, quantized accuracy, and modularization.

Inference Performance: In our LLM quantization benchmark, we prioritize the importance of selecting a quantization approach that enhances inference performance. This means our chosen setting should either increase throughput or decrease memory requirements, thereby optimizing the efficiency of the model during the inference phase.

Calibration Cost: The process of post-training quantization for LLMs are also named as calibration. The resources and time invested in calibration for LLM are crucial factors that

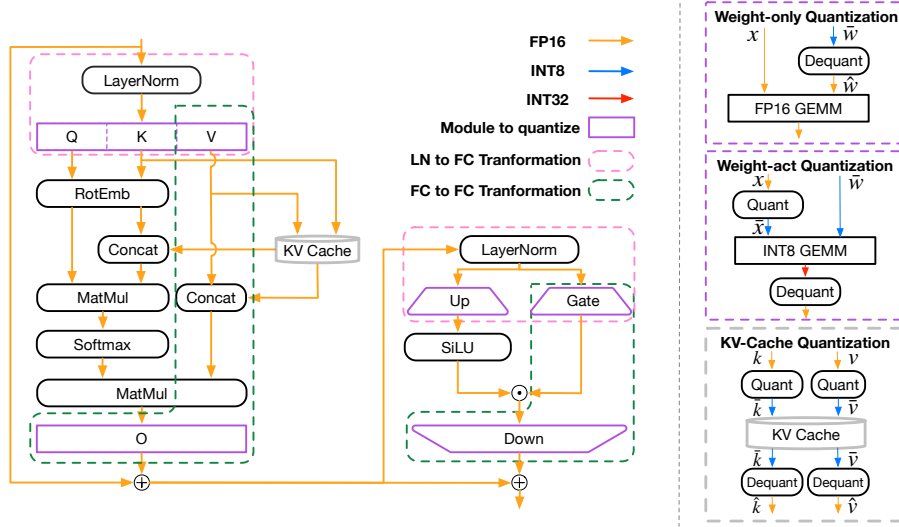


Figure 1: Inference of quantized LLMs. X , K , and V are quantized in a per-token manner with the upper and lower bounds dynamically calculated during inference. The range of W is statically calibrated before the deployment. For weight-only setting, W adopts per-group quantization and for weight-activation quantization, W uses per-channel quantization.

affect the practicality of LLM quantization. This benchmark aims to find the best pipeline to produce accurate LLMs in minimal GPUs and time.

Quantized Accuracy: In every method used to create quantized models, it’s crucial to minimize any reduction in accuracy to a tolerable degree. With this fundamental principle in mind, we are dedicated to exploring strategies that reliably preserve the performance of the model within acceptable limits.

Modularization: Recent advancements have introduced a myriad of algorithms aimed at enhancing the performance of quantized LLMs. This benchmark seeks to dissect these algorithms to their most fundamental elements, analyzing the efficacy of each component in isolation.

Guided by the aforementioned four principles, our goal is to investigate and outline optimal practices for developing quantized LLMs tailored to various scenarios and configurations.

2.2 LLM Quantization

Preliminary of Quantization. For an element x in a vector to be quantized, the process of quantization can be defined as:

$$\begin{aligned} \text{quantize: } \bar{x} &= \frac{\text{clip}(x, l, u)}{\Delta}, \Delta = \frac{u - l}{2^b - 1}, \\ \text{dequantize: } \hat{x} &= \bar{x} \cdot \Delta \end{aligned} \quad (1)$$

where u and l are the upper bound and the lower bound of the vector. b is the bit-width of the quantized vector and \bar{x} is the quantized b -bit element. if we force $u = -l$, the process can be called symmetric quantization. Otherwise, it is called asymmetric quantization. In this paper, we mainly consider asymmetric quantization. Besides that, in weight-only quantization, we employ per-group quantization, that is the weights in a group share the same Δ . In weight-activation quantization, we apply per-channel and per-token quantization for weights and activations, respectively¹. Details can be found in the subsection A.1.

Factors Influencing LLM Quantization. We categorize factors influencing LLM quantization into three dimensions: calibration data, algorithms, and target bits.

¹In this paper, the notion “wxay” is employed to represent the bit-widths “x” of weights, and the bit-widths “y” of activations. “gz” means in group-wise quantization the group size is “z”.

- **Calibration data:** Calibration data can help to evaluate the range of tensors, and then determine the quantization parameters, which is crucial for maintaining model performance post-quantization. Based on that, the impact of different corpora as calibration data warrants further investigation.
- **Algorithm:** Naive low-bit quantization always brings the accuracy drop for LLM, therefore, efficient remedies to help maintain model performance make a lot of sense. Current effective and efficient algorithms can be summarized into three types: 1) **Transformation** (Xiao et al., 2023; Lin et al., 2023; Shao et al., 2023; Wei et al., 2023b): Leveraging magnitude between weight and activation before quantization is widely used to balance quantization errors:

$$WX = (Ws)(s^{-1}X) \tag{2}$$

, where s denotes the balance factor. 2) **Clipping** (Lin et al., 2023; Shao et al., 2023; Wei et al., 2022; Du et al., 2024): Clipping some outliers with minimal impact in weights before quantization can help with range estimation and the representation of the rest in calibration:

$$W = \text{clip}(W, \alpha, \beta), l \leq \alpha < \beta \leq u \tag{3}$$

, where α and β mean clipping lower bound and upper bound, respectively. 3) **Reconstruction** (Frantar et al., 2022; Lee et al., 2023; Dettmers et al., 2023): This kind of approach employs the Hessian matrix to evaluate the quantization perturbations, and update the rest intact elements, which can be concisely represented as follows:

$$W \leftarrow W - EH^{-1} \tag{4}$$

, where E denotes the perturbation, and H^{-1} is the inverse Hessian matrix. This process is conducted incrementally during the quantization process.

- **Target bits:** The bit adopted for weight, activation, and KV cache impacts the final accuracy. Usually, the hardware-friendly bits are 2-bit, 4-bit and 8-bit. In this benchmark, we also investigate 3-bit or 6-bit to compare the potential of quantization algorithms. But for the practical deployment, 2/4/8-bit is mainly used.

Quantized inference of LLM. As shown in Figure 1, the quantization mainly targets the Linear layers with weights, i.e., the Q, K, V, and O layers in self-attention modules and the Up, Gate, and Down layer in FFN modules. Figure 1(b) presents 3 types of quantization including weight-activation quantization, weight-only quantization, and KV-cache quantization. They bring different benefits for reducing the prefill and decode latency.

2.3 Quantization Toolkit

To achieve the modular comparison of the different quantization dimensions aforementioned, and to consolidate best practices into an end-to-end pipeline, we have designed and developed a quantization toolkit named LLMC. This toolkit is capable of accommodating multiple quantization configurations using a variety of algorithmic techniques. The models produced by LLMC are designed for seamless deployment across a diverse range of hardware platforms. Presently, LLMC supports over ten algorithms, is compatible with over eight models, is flexible to extend the support of any transformer-based LLMs, and facilitates deployment on three types of inference engines including LightLLM (ModelTC, 2023), TensorRT-LLM (Nvidia, 2023) and PPL-LLM (OpenPPL, 2023).

3 LLM-QBench

Under the principles in subsection 2.1, powered by our quantization toolkit LLMC, in this section, we explore the best practice for quantizing large language models from the aspect of calibration data, quantization algorithm, and target bit.

Calib. Data			GPTQ		AWQ		SmoothQuant		OS+		OmniQuant	
WikiText2	C4	Pile (val)	WikiText2	C4	WikiText2	C4	WikiText2	C4	WikiText2	C4	WikiText2	C4
✓			11.93	-	2.19e5	-	140.74	-	84.39	-	9.86	-
	✓		-	18.15	-	1.68e5	-	109.41	-	82.29	-	13.73
		✓	15.85	19.90	2.18e5	1.65e5	178.47	119.11	95.22	85.59	11.55	13.96

Table 1: Impact of calibration data on performance across algorithms. We evaluate the performance of various algorithms using different calibration datasets (WikiText2, C4, and Pile) and report the PPL (\downarrow) on the WikiText2 and C4 validation sets.

3.1 Experimental Settings

We first illustrate our experiment settings, more details can be found in the [subsection A.1](#).

Models. To demonstrate the generability of our benchmark, We access performance on LLAMA-2 (Touvron et al., 2023) family, spanning model sizes from 7B to 70B for general language tasks. To broaden the scope of our evaluation benchmarks, we also benchmark on ChatGLM (Zeng et al., 2023) for long context abilities, CodeLLAMA (Roziere et al., 2023) for coding tasks and WizardMath (Luo et al., 2023) for mathematical problems.

Datasets. We categorize the datasets into upstream datasets and downstream datasets. For the upstream datasets, we employ WikiText2 (Foundation) and C4 (Raffel et al., 2019) dataset with the perplexity metric for evaluation, since perplexity can stably reflect the LLM’s performance (Dettmers & Zettlemoyer, 2023). For the downstream tasks, we select examination tasks including MMLU (Hendrycks et al., 2021) and ARC-e (Clark et al., 2018), knowledge task BoolQ (Clark et al., 2019), understanding task Lambada (Paperno et al., 2016), reasoning tasks including PIQA (Bisk et al., 2020), HellaSwag (Zellers et al., 2019) and GSM8K (Cobbe et al., 2021), coding tasks HumanEval (Chen et al., 2021) and MBPP (Austin et al., 2021), and the long context evaluation LongBench (Bai et al., 2023).

Hardware. Benefiting from the versatility of our tool, we can efficiently and conveniently quantize LLMs to support multiple inference backends and hardware platforms. In this paper, we mainly measured the inference efficiency of low-bit kernel on NVIDIA server and edge GPUs with NVIDIA’s TensorRT-LLM (Nvidia, 2023) framework.

3.2 Impact of Calibration Data

Initially, we examine the influence of calibration data on the accuracy of quantization, as illustrated by [Table 1](#). It is evident that calibration data affects all algorithms. To attain optimal accuracy, it is crucial to gather domain-specific data for domain-specific models and collect diverse data for the general models.

Takeaway 1.

- For LLMs aimed to solve general tasks, we need to utilize the diverse data across various tasks it will face.
- For specific-purpose LLM, it would be better to calibrate the model with the same domain.

3.3 Quantization Algorithm

Following the principles of modularization, we deconstruct the techniques behind existing algorithms. Through a comprehensive and unbiased experimental comparison, we aim to derive insights critical for developing an optimally combined quantization pipeline.

As outlined in [Table 2](#), we summarize the different strategies transformation, clipping, and reconstruction techniques, define their behavior and analyze their calibration cost accordingly. We evaluate these techniques on LLAMA-2 models of 7B, 13B, and 70B sizes, under both weight-only and weight-activation quantization scenarios. Here the 2-bit weight-only experiment of 70B LLAMA-2 is chosen as a representative in the main text. More results are illustrated in [subsection A.2](#).

Clipping. From the [Table 3](#), we find that searching for the clipping value asymmetrically is the most effective strategy for optimizing accuracy. This indicates that selecting an appropriate weight range can significantly reduce weight quantization error. Therefore,

Technique	Category	Strategy	Eq. Trans.	Calib. Cost	Algorithm	Alias
Transformation	<i>Rule-based</i>	$s = \max(X ^\gamma) / \max(W ^{1-\gamma}), \gamma = 0.5, 0.75$	✓	Low	SmoothQuant	TR
	<i>Search-based</i>	v1: $s = \max(X ^\gamma) / \max(W ^{1-\gamma}), \gamma \in [0, 1]$	✓	Medium	AWQ	TS-v1
		v2: $s = \max(1.0, \max(X))$	✓	Medium	OS+	TS-v2
	<i>Learning-based</i>	$s = \arg \min_s \mathcal{L}$	✓	High	OmniQuant	TL
Clipping	<i>Min-max</i>	$\alpha = \min(W), \beta = \max W$	✓	Low	SmoothQuant, OS+, GPTQ	CM
	<i>Search-based</i>	symmetric: $\alpha = \beta \in (0, \max(W))$	✗	Medium	AWQ	CS-sym
		asymmetric: $\alpha, \beta \in (0, \max(W))$	✗	Medium	-	CS-asym
	<i>Learning-based</i>	$\alpha, \beta = \arg \min_{\alpha, \beta} \mathcal{L}$	✗	High	OmniQuant	CL
Reconstruction	<i>Hessian-based</i>	$W \leftarrow W - EH^{-1}$	✗	Medium	GPTQ	RH

Table 2: Detailed comparison of the decomposed quantization techniques and strategies. **Eq. Trans.** indicates whether the algorithm is an equivalent transformation. **Calib. Cost** represents the level of required GPU resources and time for calibration. γ is the scaling factor, and \mathcal{L} is the loss function.

we also adopt this strategy for the weight-activation quantization. Clipping should be fully utilized in the pipeline of best practices. What’s more, initialized from the asymmetric clipping, the accuracy can be boosted by further learning. This good initialization contributes to a fast convergence.

Reconstruction. GPTQ (Frantar et al., 2022) reconstruction involves the non-equivalent transformation of weights on the channel dimension, hindering simultaneous optimization of weights and clip values. Pre-reconstruction weight clip yields suboptimal results due to weight changes. If reconstruction precedes clip value search, initial quantization parameters won’t match the updated ones. Moreover, when paired with an equivalent transformation, it yields minimal benefits. This limitation may stem from the alteration of gradients and the disruption of assumptions regarding Hessian information. Furthermore, it requires an extended calibration period. Therefore, reconstruction may not be considered a best practice.

Transformation. The transformation technique utilizes the linear operation to reduce the outlier problem in LLM or preserve the important weights. for both the weight-only and weight-activation quantization, such equivalent transformation brings an accuracy improvement, especially for the activations. From the table, we can infer that manually setting the scaling number is rigid and may not help in all scenarios. On the contrary, a suitable search for the transformation scale s is effective. There are different search strategies and both help a lot at improving the accuracy. A learning process can be further adopted with a pre-searched range. Fortunately, with the support of fast pre-search, the calibration can achieve learning with fewer epochs.

Calibration cost for each strategy. In the analysis of calibration costs detailed in Table 4, we observe that within the suite of transformation techniques, the search-based (v1) strategy requires roughly 10 minutes, making it twice as fast as the (v2) strategy. While rule-based transformations are quicker, they often fall short of achieving acceptable accuracy levels. On the other hand, learning-based transformation methods incur a considerable increase in time to attain satisfactory accuracy levels. However, initializing the learning process with pre-searched values can halve the number of epochs required and yield higher accuracy. Regarding clipping methods, employing direct min-max value clipping is time-efficient but typically results in significant accuracy loss. The search-based clipping method, whether using asymmetric or symmetric ranges, proves efficient, requiring only about 20 minutes. Yet, when applying a learning-based approach to clipping, the calibration time can extend to nearly 7 hours. Therefore, a combined approach of the search-based transformation v1 and search-based asymmetric clipping emerges as the most effective in balancing accuracy and efficiency. Furthermore, initiating with pre-searched values and conducting additional learning for a few epochs may offer further accuracy improvements.

Method	PPL ↓			Accuracy (%) ↑					
	WikiText2	C4	Avg.	MMLU*	ARC-e*	BoolQ*	HellaSwag*	PIQA*	Avg.
Full Prec.	3.32	5.71	4.52	70.91	88.44	83.33	80.00	83.50	81.24
TR	7.56	10.79	9.18	51.44	38.19	59.00	69.20	76.50	58.87
TS-v1	6.69	9.41	8.05	40.21	45.73	73.33	67.60	77.50	60.87
TS-v2	7.25	10.42	8.83	49.63	48.74	62.67	70.00	78.50	61.91
-----	-----	-----	-----	-----	-----	-----	-----	-----	-----
CM	10.32	15.16	12.74	34.45	34.67	54.00	62.40	73.50	51.80
CS-sym	7.2e4	6.5e4	6.9e4	27.79	26.63	41.67	25.60	51.50	34.64
CS-asym	5.67	8.26	6.97	53.44	69.85	78.67	72.80	78.00	70.55
CL	6.13	8.62	7.38	49.59	47.24	75.67	72.80	79.50	64.96
-----	-----	-----	-----	-----	-----	-----	-----	-----	-----
RH	6.68	9.40	8.04	54.65	42.21	70.33	67.20	77.00	62.28
TS-v1+RH	6.69	9.45	8.07	50.00	42.71	73.67	65.60	73.50	61.10
TS-v1+CS-sym	7.1e4	6.5e4	6.8e4	27.79	26.63	41.67	25.60	51.00	34.54
TS-v1+CS-asym	5.24	7.73	6.49	59.52	77.89	82.33	74.80	82.00	75.31
TS-v1+CL w/ CS-asym init.	5.24	7.70	6.47	59.40	77.25	82.39	75.46	78.51	74.60

Table 3: Ablation results of LLaMA-2-70B weight-only (w2a16g64) quantization. * means the subset of the corresponding dataset.

TR	TS	TS	TL	TL	TL	CS	CL	TS-v1	TL	TS-v1 + CL	TL w/ TS-v1 init.	RH
-v1	-v2	w/ ones init.	w/ TR init.	w/ TS-v1 init.	-asym	+CS-asym	+CL	w/ CS-asym init.	+CL w/ CS-asym init.			
Time	~ 0.08h	~ 0.2h	~ 0.5h	~ 7.3h	~ 7.3h	~ 4h	~ 0.4h ~ 6.8h	~ 0.6h	~ 8.3h	~ 3.5h	~ 4.4h	~ 0.6h

Table 4: Calibration cost on LLaMA-2-70B of different strategies in Table 2. Ones init. means we use a vector of ones as the start point of s before learning.

Takeaway 2.

- Search-based clipping and transformation are optimal solutions for balancing the calibration cost and accuracy. The searched values benefit initializing the learning-based solutions.
- Incorrect clipping easily leads to an accuracy crash. Asymmetric clipping is simple yet effective for improving the accuracy.
- Transformation searching influences both the calibration efficiency and quantized accuracy. The v1 strategy in Table 2 enjoys a good tradeoff between them.

3.4 Target Bits

Fixed-precision. In the experimental results presented in subsection 3.3, we observed that both 2-bit weight-only quantization and w4a4 weight-activation quantization experienced over a 20% degradation in accuracy. This significant reduction in performance limits their practical utility. In contrast, 3-bit weight-only and w6a6 weight-activation quantization were primarily evaluated to assess algorithm capabilities and cannot achieve practical hardware acceleration. Consequently, we recommend the 4-bit weight-only, w4a8, or w8a8 weight-activation quantization approaches as they strike a balance between maintaining accuracy and enhancing inference speed. Furthermore, quantization of the Key-Value (KV) cache is proposed as a method to decrease memory usage. In Table 21 and Table 5, we assessed the accuracy impact of 2-bit (per-group quantization with a group size of 8), 4-bit (per-group quantization with a group size of 8), and 8-bit (per-tensor) KV cache quantization. The results indicate that 2-bit KV cache quantization leads to a substantial loss in accuracy, while 4-bit KV cache quantization, with its finer granularity, performs comparably to 8-bit KV cache quantization with a coarser group size. Both the 4-bit and 8-bit configurations closely approximate the performance of FP16 at the code generation task and long-context understanding task. Hence, for KV cache quantization, a 4-bit per-group approach with a group size of 8 is recommended.

Mixed-precision. As presented in our experiments, quantizing LLMs into ultra-low precision without significant accuracy loss is difficult. A viable remedy is to employ mix-precision quantization. For mix-precision, we only evaluate accuracy for theoretically hardware-friendly strategies since there are no open-access fast kernels to evaluate inference.

Model	KV Cache Prec.	Accuracy (%) \uparrow				
		NarrativeQA	QASPER	MultiFieldQA-en	MultiFieldQA-zh	Avg.
ChatGLM3-6B-32k	Full Prec.	25.93	43.35	51.57	62.36	45.80
	int8	25.74	43.57	51.81	62.48	45.90
	int4	26.13	43.43	51.63	61.04	45.56
	int2	1.89	4.68	3.13	1.08	2.70

Table 5: KV cache quantization results on Single-Document QA from LongBench Bai et al. (2023)

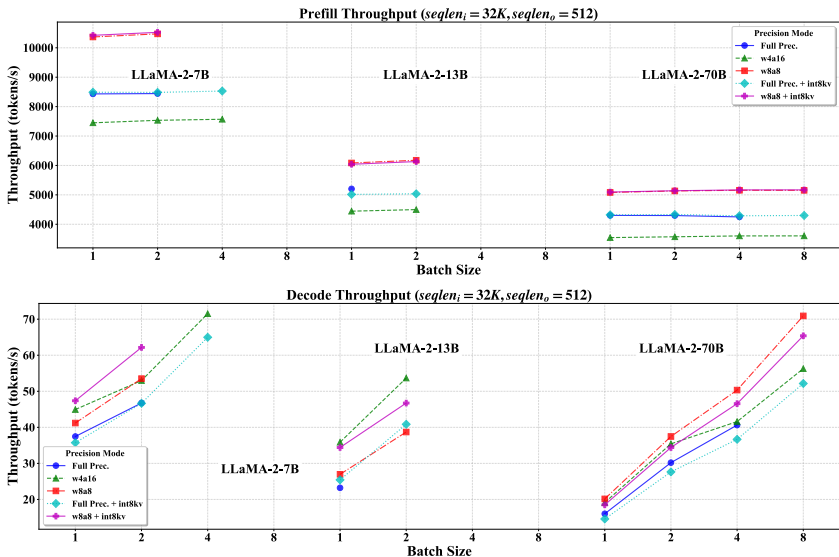


Figure 2: Inference speed of 7B, 13B and 70B LLAMA-2 models on NVIDIA A100 GPU. (Input sequence length: 32K, Output sequence length: 512)

As shown in Table 22, Table 23, and Table 24, for weight-only quantization, employing Hessain disturbance as bit allocate strategy outperforms others. High-bit quantization benefits from lower mixture rates, while low-bit requires more full-precision weights in small LLMs for better performance. For weight-activation quantization, dynamic bit allocation with slower inference speed and higher computational overhead during inference gains more accuracy improvements rather than static strategy, even though the latter uses a double mixture rate. Details are presented in the subsection A.6.

Inference Speed. To assess the practical benefits of different quantization approaches, we conducted evaluations using NVIDIA’s cloud (SMX 80G A100) and edge (Drive Orin) GPUs, alongside the official inference library, TensorRT-LLM. Part of our results, as depicted in Figure 2, highlight the throughput improvements achieved through TensorRT-LLM-supported quantization schemes for models with 32,000 input tokens and 512 output tokens. The findings indicate that quantization with 8-bit weights and activations enhances the prefill stage’s speed by 20%-30% and the decode stage by 40%-60%. In contrast, 4-bit weight-only quantization reduces the prefill speed by 10% but increases the decode speed by 40%-60%. It’s important to note that these acceleration rates tend to diminish for larger models. Besides, 8-bit KV cache quantization has minimal impact on prefill times and slightly reduces decoding throughput for very large models, such as those with 70B model. Results for more models and hardware can be found in subsection A.5.

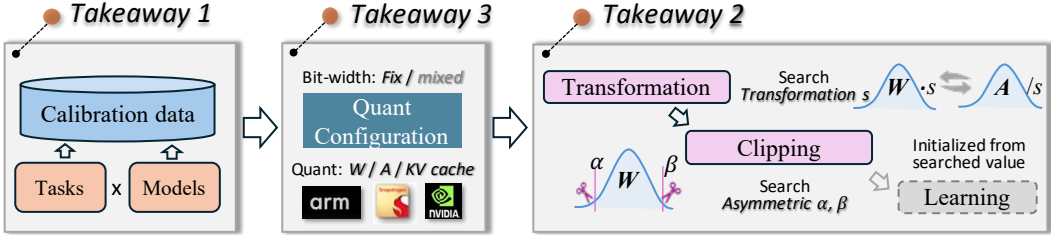


Figure 3: The best practice of PTQ pipeline for LLMs.

Method	Accuracy (%) ↑					
	MMLU	ARC-e	BoolQ	HellaSwag	PIQA	Avg.
Full Prec.	70.91	88.44	83.33	80.00	83.50	81.24
Naive	31.72	30.69	53.88	66.83	72.14	51.05
GPTQ	50.50	41.09	76.39	69.04	75.41	62.49
AWQ	24.46	26.46	37.83	24.60	50.87	32.84
OmniQuant	49.27	47.80	78.07	72.79	77.91	65.17
TS-v1+CS-asym	57.91	80.07	83.91	75.98	78.67	75.31
TS-v1+CL w/ CS-asym init.	59.40	77.25	82.39	75.46	78.51	74.60

Table 6: Main results of LLaMA-2-70B (w2a16g64) weight-only quantization.

#Bits	Method	CodeLlama-7b		WizardMath-7b	
		HumanEval(Pass@1(%) †)		GSM8K-100(Acc.(%) †)	
Full Prec.	-	31.10		51.00	
	Naive	26.83		32.00	
w3a16	TS-v1+CL w/ CS-asym init.	23.17		38.00	
	TS-v1+CL w/ CS-asym init.†	28.05		46.00	

Table 7: Main results of code and math analyses. † indicates calibration with the corresponding data. For the CodeLlama-7b model, we use a sample of 10 instances from the MBPP and HumanEval datasets, respectively. Similarly, for the WizardMath-7b model, we sample 10 instances from the MATH and GSM8K datasets, respectively .

Takeaway 3.

- For fixed-precision, considering the principle of inference speed and quantized accuracy, 4-bit weight-only quantization, w4a8/w8a8 weight-activation quantization, and 4-bit KV cache quantization with group size=8 are promising settings. Larger models can tolerate lower bit for weights.
- Weight quantization benefits decoding speed and harms prefill speed. Weight-activation quantization benefits both the prefill and decode speed, and KV cache quantization only brings little speedup for small models but helps reduce memory consumption for long context.
- For mixed precision (**specialized kernel requirements**), hessian-based metrics excel in determining the precision for weight quantization, while dynamic magnitude-based strategies with non-negligible overhead are better for enhancing accuracy toward weight activation quantization.

3.5 Best Practice of LLM PTQ pipeline

Based on the takeaways distilled from the above exploration, we summarize the best practice of PTQ pipeline for LLM. As depicted in Figure 3, first, we should collect the best calibration data according to the task and model under the guide of Takeaway 1. Then the bit-width and quantization scheme could be determined considering the Takeaway 3. Finally, the calibration process can be conducted using the algorithm pipeline based on Takeaway 2. The results in Table 6 and Table 7 of general-purpose model LLaMA-2-70B and specific-domain code model CodeLLaMA-7b and math model WizardMath-7b proved the effectiveness, especially for maintaining high accuracy. More experimental results on other models and

datasets to validate our best practice for decent performance and efficient inference can be found in [subsection A.3](#).

4 Conclusion

In this study, we have undertaken a comprehensive benchmarking of decomposed quantization techniques for large language models (LLMs), leading to the identification of best practices that balance calibration costs, accuracy, and efficiency. Furthermore, we introduce LLMC, a toolkit designed to empower the research and development community. Models optimized through our recommended practices and toolkit are readily deployable across a variety of hardware platforms, enhancing accessibility and applicability in diverse computational environments.

References

- Saleh Ashkboos, Iliia Markov, Elias Frantar, Tingxuan Zhong, Xincheng Wang, Jie Ren, Torsten Hoefler, and Dan Alistarh. Quik: Towards end-to-end 4-bit inference on generative large language models, 2023.
- Jacob Austin, Augustus Odena, Maxwell Nye, Maarten Bosma, Henryk Michalewski, David Dohan, Ellen Jiang, Carrie Cai, Michael Terry, Quoc Le, et al. Program synthesis with large language models. *arXiv preprint arXiv:2108.07732*, 2021.
- Yushi Bai, Xin Lv, Jiajie Zhang, Hongchang Lyu, Jiankai Tang, Zhidian Huang, Zhengxiao Du, Xiao Liu, Aohan Zeng, Lei Hou, Yuxiao Dong, Jie Tang, and Juanzi Li. Longbench: A bilingual, multitask benchmark for long context understanding. *arXiv preprint arXiv:2308.14508*, 2023.
- Yash Bhalgat, Jinwon Lee, Markus Nagel, Tijmen Blankevoort, and Nojun Kwak. Lsq+: Improving low-bit quantization through learnable offsets and better initialization, 2020.
- Yonatan Bisk, Rowan Zellers, Ronan Le Bras, Jianfeng Gao, and Yejin Choi. Piqa: Reasoning about physical commonsense in natural language. In *Thirty-Fourth AAAI Conference on Artificial Intelligence*, 2020.
- Jerry Chee, Yaohui Cai, Volodymyr Kuleshov, and Christopher De Sa. Quip: 2-bit quantization of large language models with guarantees, 2024.
- Mark Chen, Jerry Tworek, Heewoo Jun, Qiming Yuan, Henrique Ponde de Oliveira Pinto, Jared Kaplan, Harri Edwards, Yuri Burda, Nicholas Joseph, Greg Brockman, Alex Ray, Raul Puri, Gretchen Krueger, Michael Petrov, Heidy Khlaaf, Girish Sastry, Pamela Mishkin, Brooke Chan, Scott Gray, Nick Ryder, Mikhail Pavlov, Alethea Power, Lukasz Kaiser, Mohammad Bavarian, Clemens Winter, Philippe Tillet, Felipe Petroski Such, Dave Cummings, Matthias Plappert, Fotios Chantzis, Elizabeth Barnes, Ariel Herbert-Voss, William Hebgen Guss, Alex Nichol, Alex Paino, Nikolas Tezak, Jie Tang, Igor Babuschkin, Suchir Balaji, Shantanu Jain, William Saunders, Christopher Hesse, Andrew N. Carr, Jan Leike, Josh Achiam, Vedant Misra, Evan Morikawa, Alec Radford, Matthew Knight, Miles Brundage, Mira Murati, Katie Mayer, Peter Welinder, Bob McGrew, Dario Amodei, Sam McCandlish, Ilya Sutskever, and Wojciech Zaremba. Evaluating large language models trained on code. 2021.
- Christopher Clark, Kenton Lee, Ming-Wei Chang, Tom Kwiatkowski, Michael Collins, and Kristina Toutanova. Boolq: Exploring the surprising difficulty of natural yes/no questions, 2019.
- Peter Clark, Isaac Cowhey, Oren Etzioni, Tushar Khot, Ashish Sabharwal, Carissa Schoenick, and Oyvind Tafjord. Think you have solved question answering? try arc, the ai2 reasoning challenge. *arXiv:1803.05457v1*, 2018.

- Karl Cobbe, Vineet Kosaraju, Mohammad Bavarian, Mark Chen, Heewoo Jun, Lukasz Kaiser, Matthias Plappert, Jerry Tworek, Jacob Hilton, Reiichiro Nakano, Christopher Hesse, and John Schulman. Training verifiers to solve math word problems. *arXiv preprint arXiv:2110.14168*, 2021.
- Tim Dettmers and Luke Zettlemoyer. The case for 4-bit precision: k-bit inference scaling laws, 2023.
- Tim Dettmers, Mike Lewis, Younes Belkada, and Luke Zettlemoyer. Llm. int8 (): 8-bit matrix multiplication for transformers at scale. *arXiv preprint arXiv:2208.07339*, 2022.
- Tim Dettmers, Ruslan Svirschevski, Vage Egiazarian, Denis Kuznedelev, Elias Frantar, Saleh Ashkboos, Alexander Borzunov, Torsten Hoefler, and Dan Alistarh. Spqr: A sparse-quantized representation for near-lossless llm weight compression. *arXiv preprint arXiv:2306.03078*, 2023.
- Dayou Du, Yijia Zhang, Shijie Cao, Jiaqi Guo, Ting Cao, Xiaowen Chu, and Ningyi Xu. Bitdistiller: Unleashing the potential of sub-4-bit llms via self-distillation, 2024.
- Vage Egiazarian, Andrei Panferov, Denis Kuznedelev, Elias Frantar, Artem Babenko, and Dan Alistarh. Extreme compression of large language models via additive quantization, 2024.
- Steven K. Esser, Jeffrey L. McKinstry, Deepika Bablani, Rathinakumar Appuswamy, and Dharmendra S. Modha. Learned step size quantization, 2020.
- Wikimedia Foundation. Wikimedia downloads. URL <https://dumps.wikimedia.org>.
- Elias Frantar, Saleh Ashkboos, Torsten Hoefler, and Dan Alistarh. Gptq: Accurate post-training quantization for generative pre-trained transformers. *arXiv preprint arXiv:2210.17323*, 2022.
- Leo Gao, Stella Biderman, Sid Black, Laurence Golding, Travis Hoppe, Charles Foster, Jason Phang, Horace He, Anish Thite, Noa Nabeshima, Shawn Presser, and Connor Leahy. The Pile: An 800gb dataset of diverse text for language modeling. *arXiv preprint arXiv:2101.00027*, 2020.
- Ruihao Gong, Xianglong Liu, Shenghu Jiang, Tianxiang Li, Peng Hu, Jiazhen Lin, Fengwei Yu, and Junjie Yan. Differentiable soft quantization: Bridging full-precision and low-bit neural networks. In *The IEEE International Conference on Computer Vision (ICCV)*, October 2019.
- Dan Hendrycks, Collin Burns, Steven Basart, Andy Zou, Mantas Mazeika, Dawn Song, and Jacob Steinhardt. Measuring massive multitask language understanding. *Proceedings of the International Conference on Learning Representations (ICLR)*, 2021.
- Jung Hwan Heo, Jeonghoon Kim, Beomseok Kwon, Byeongwook Kim, Se Jung Kwon, and Dongsoo Lee. Rethinking channel dimensions to isolate outliers for low-bit weight quantization of large language models, 2023.
- Divyansh Jhunjhunwala, Advait Gadhikar, Gauri Joshi, and Yonina C. Eldar. Adaptive quantization of model updates for communication-efficient federated learning, 2021.
- Sehoon Kim, Coleman Hooper, Amir Gholami, Zhen Dong, Xiuyu Li, Sheng Shen, Michael W. Mahoney, and Kurt Keutzer. Squeezellm: Dense-and-sparse quantization, 2024.
- Changhun Lee, Jungyu Jin, Taesu Kim, Hyungjun Kim, and Eunhyeok Park. Owq: Lessons learned from activation outliers for weight quantization in large language models. *arXiv preprint arXiv:2306.02272*, 2023.
- Yuhang Li, Ruihao Gong, Xu Tan, Yang Yang, Peng Hu, Qi Zhang, Fengwei Yu, Wei Wang, and Shi Gu. Brecq: Pushing the limit of post-training quantization by block reconstruction, 2021.

- Ji Lin, Jiaming Tang, Haotian Tang, Shang Yang, Xingyu Dang, and Song Han. Awq: Activation-aware weight quantization for llm compression and acceleration. *arXiv preprint arXiv:2306.00978*, 2023.
- Jing Liu, Ruihao Gong, Xiuying Wei, Zhiwei Dong, Jianfei Cai, and Bohan Zhuang. Qllm: Accurate and efficient low-bitwidth quantization for large language models, 2024.
- Zechun Liu, Barlas Oguz, Changsheng Zhao, Ernie Chang, Pierre Stock, Yashar Mehdad, Yangyang Shi, Raghuraman Krishnamoorthi, and Vikas Chandra. Llm-qat: Data-free quantization aware training for large language models, 2023.
- Haipeng Luo, Qingfeng Sun, Can Xu, Pu Zhao, Jianguang Lou, Chongyang Tao, Xiubo Geng, Qingwei Lin, Shifeng Chen, and Dongmei Zhang. Wizardmath: Empowering mathematical reasoning for large language models via reinforced evol-instruct. *arXiv preprint arXiv:2308.09583*, 2023.
- ModelTC. Lightllm. <https://github.com/ModelTC/lightllm>, 2023.
- Markus Nagel, Marios Fournarakis, Rana Ali Amjad, Yelysei Bondarenko, Mart van Baalen, and Tijmen Blankevoort. A white paper on neural network quantization, 2021.
- Nvidia. Tensorrt-llm. <https://github.com/NVIDIA/TensorRT-LLM>, 2023.
- OpenAI, Josh Achiam, Steven Adler, Sandhini Agarwal, Lama Ahmad, Ilge Akkaya, Florencia Leoni Aleman, Diogo Almeida, Janko Altmenschmidt, Sam Altman, Shyamal Anadkat, Red Avila, Igor Babuschkin, Suchir Balaji, Valerie Balcom, Paul Baltescu, Haiming Bao, Mohammad Bavarian, Jeff Belgum, Irwan Bello, Jake Berdine, Gabriel Bernadett-Shapiro, Christopher Berner, Lenny Bogdonoff, Oleg Boiko, Madelaine Boyd, Anna-Luisa Brakman, Greg Brockman, Tim Brooks, Miles Brundage, Kevin Button, Trevor Cai, Rosie Campbell, Andrew Cann, Brittany Carey, Chelsea Carlson, Rory Carmichael, Brooke Chan, Che Chang, Fotis Chantzis, Derek Chen, Sully Chen, Ruby Chen, Jason Chen, Mark Chen, Ben Chess, Chester Cho, Casey Chu, Hyung Won Chung, Dave Cummings, Jeremiah Currier, Yunxing Dai, Cory Decareaux, Thomas Degry, Noah Deutsch, Damien Deville, Arka Dhar, David Dohan, Steve Dowling, Sheila Dunning, Adrien Ecoffet, Atty Eleti, Tyna Eloundou, David Farhi, Liam Fedus, Niko Felix, Simón Posada Fishman, Juston Forte, Isabella Fulford, Leo Gao, Elie Georges, Christian Gibson, Vik Goel, Tarun Gogineni, Gabriel Goh, Rapha Gontijo-Lopes, Jonathan Gordon, Morgan Grafstein, Scott Gray, Ryan Greene, Joshua Gross, Shixiang Shane Gu, Yufei Guo, Chris Hallacy, Jesse Han, Jeff Harris, Yuchen He, Mike Heaton, Johannes Heidecke, Chris Hesse, Alan Hickey, Wade Hickey, Peter Hoeschele, Brandon Houghton, Kenny Hsu, Shengli Hu, Xin Hu, Joost Huizinga, Shantanu Jain, Shawn Jain, Joanne Jang, Angela Jiang, Roger Jiang, Haozhun Jin, Denny Jin, Shino Jomoto, Billie Jonn, Heewoo Jun, Tomer Kaftan, Łukasz Kaiser, Ali Kamali, Ingmar Kanitscheider, Nitish Shirish Keskar, Tabarak Khan, Logan Kilpatrick, Jong Wook Kim, Christina Kim, Yongjik Kim, Jan Hendrik Kirchner, Jamie Kiros, Matt Knight, Daniel Kokotajlo, Łukasz Kondraciuk, Andrew Kondrich, Aris Konstantinidis, Kyle Kosic, Gretchen Krueger, Vishal Kuo, Michael Lampe, Ikai Lan, Teddy Lee, Jan Leike, Jade Leung, Daniel Levy, Chak Ming Li, Rachel Lim, Molly Lin, Stephanie Lin, Mateusz Litwin, Theresa Lopez, Ryan Lowe, Patricia Lue, Anna Makanju, Kim Malfacini, Sam Manning, Todor Markov, Yaniv Markovski, Bianca Martin, Katie Mayer, Andrew Mayne, Bob McGrew, Scott Mayer McKinney, Christine McLeavey, Paul McMillan, Jake McNeil, David Medina, Aalok Mehta, Jacob Menick, Luke Metz, Andrey Mishchenko, Pamela Mishkin, Vinnie Monaco, Evan Morikawa, Daniel Mossing, Tong Mu, Mira Murati, Oleg Murk, David Mély, Ashvin Nair, Reiichiro Nakano, Rajeev Nayak, Arvind Neelakantan, Richard Ngo, Hyeonwoo Noh, Long Ouyang, Cullen O’Keefe, Jakub Pachocki, Alex Paino, Joe Palermo, Ashley Pantuliano, Giambattista Parascandolo, Joel Parish, Emy Parparita, Alex Passos, Mikhail Pavlov, Andrew Peng, Adam Perelman, Filipe de Avila Belbute Peres, Michael Petrov, Henrique Ponde de Oliveira Pinto, Michael, Pokornyy, Michelle Pokrass, Vitchyr H. Pong, Tolly Powell, Alethea Power, Boris Power, Elizabeth Proehl, Raul Puri, Alec Radford, Jack Rae, Aditya Ramesh, Cameron Raymond, Francis Real, Kendra Rimbach, Carl Ross, Bob Rotsted, Henri Roussez, Nick Ryder, Mario Saltarelli, Ted Sanders, Shibani Santurkar, Girish Sastry, Heather Schmidt, David Schnurr,

John Schulman, Daniel Selsam, Kyla Sheppard, Toki Sherbakov, Jessica Shieh, Sarah Shoker, Pranav Shyam, Szymon Sidor, Eric Sigler, Maddie Simens, Jordan Sitkin, Katarina Slama, Ian Sohl, Benjamin Sokolowsky, Yang Song, Natalie Staudacher, Felipe Petroski Such, Natalie Summers, Ilya Sutskever, Jie Tang, Nikolas Tezak, Madeleine B. Thompson, Phil Tillet, Amin Tootoonchian, Elizabeth Tseng, Preston Tuggle, Nick Turley, Jerry Tworek, Juan Felipe Cerón Uribe, Andrea Vallone, Arun Vijayvergiya, Chelsea Voss, Carroll Wainwright, Justin Jay Wang, Alvin Wang, Ben Wang, Jonathan Ward, Jason Wei, CJ Weinmann, Akila Welihinda, Peter Welinder, Jiayi Weng, Lilian Weng, Matt Wiethoff, Dave Willner, Clemens Winter, Samuel Wolrich, Hannah Wong, Lauren Workman, Sherwin Wu, Jeff Wu, Michael Wu, Kai Xiao, Tao Xu, Sarah Yoo, Kevin Yu, Qiming Yuan, Wojciech Zaremba, Rowan Zellers, Chong Zhang, Marvin Zhang, Shengjia Zhao, Tianhao Zheng, Juntang Zhuang, William Zhuk, and Barret Zoph. Gpt-4 technical report, 2024.

OpenPPL. Ppl-llm. <https://github.com/openppl-public/ppl.nn.llm>, 2023.

Denis Paperno, Germán Kruszewski, Angeliki Lazaridou, Ngoc Quan Pham, Raffaella Bernardi, Sandro Pezzelle, Marco Baroni, Gemma Boleda, and Raquel Fernandez. The LAMBADA dataset: Word prediction requiring a broad discourse context. In *Proceedings of the 54th Annual Meeting of the Association for Computational Linguistics (Volume 1: Long Papers)*, pp. 1525–1534, Berlin, Germany, August 2016. Association for Computational Linguistics. URL <http://www.aclweb.org/anthology/P16-1144>.

Colin Raffel, Noam Shazeer, Adam Roberts, Katherine Lee, Sharan Narang, Michael Matena, Yanqi Zhou, Wei Li, and Peter J. Liu. Exploring the limits of transfer learning with a unified text-to-text transformer. *arXiv e-prints*, 2019.

Baptiste Roziere, Jonas Gehring, Fabian Gloeckle, Sten Sootla, Itai Gat, Xiaoqing Ellen Tan, Yossi Adi, Jingyu Liu, Tal Remez, Jérémy Rapin, et al. Code llama: Open foundation models for code. *arXiv preprint arXiv:2308.12950*, 2023.

Wenqi Shao, Mengzhao Chen, Zhaoyang Zhang, Peng Xu, Lirui Zhao, Zhiqian Li, Kaipeng Zhang, Peng Gao, Yu Qiao, and Ping Luo. Omniquant: Omnidirectionally calibrated quantization for large language models. *arXiv preprint arXiv:2308.13137*, 2023.

Sheng Shen, Zhen Dong, Jiayu Ye, Linjian Ma, Zhewei Yao, Amir Gholami, Michael W Mahoney, and Kurt Keutzer. Q-bert: Hessian based ultra low precision quantization of bert. In *Proceedings of the AAAI Conference on Artificial Intelligence*, pp. 8815–8821, 2020.

Hugo Touvron, Louis Martin, Kevin Stone, Peter Albert, Amjad Almahairi, Yasmine Babaei, Nikolay Bashlykov, Soumya Batra, Prajjwal Bhargava, Shruti Bhosale, Dan Bikel, Lukas Blecher, Cristian Canton Ferrer, Moya Chen, Guillem Cucurull, David Esiobu, Jude Fernandes, Jeremy Fu, Wenyin Fu, Brian Fuller, Cynthia Gao, Vedanuj Goswami, Naman Goyal, Anthony Hartshorn, Saghar Hosseini, Rui Hou, Hakan Inan, Marcin Kardas, Viktor Kerkez, Madian Khabsa, Isabel Kloumann, Artem Korenev, Punit Singh Koura, Marie-Anne Lachaux, Thibaut Lavril, Jenya Lee, Diana Liskovich, Yinghai Lu, Yuning Mao, Xavier Martinet, Todor Mihaylov, Pushkar Mishra, Igor Molybog, Yixin Nie, Andrew Poulton, Jeremy Reizenstein, Rashi Rungta, Kalyan Saladi, Alan Schelten, Ruan Silva, Eric Michael Smith, Ranjan Subramanian, Xiaoqing Ellen Tan, Binh Tang, Ross Taylor, Adina Williams, Jian Xiang Kuan, Puxin Xu, Zheng Yan, Iliyan Zarov, Yuchen Zhang, Angela Fan, Melanie Kambadur, Sharan Narang, Aurelien Rodriguez, Robert Stojnic, Sergey Edunov, and Thomas Scialom. Llama 2: Open foundation and fine-tuned chat models, 2023.

Albert Tseng, Jerry Chee, Qingyao Sun, Volodymyr Kuleshov, and Christopher De Sa. Quip#: Even better llm quantization with hadamard incoherence and lattice codebooks, 2024.

Mart van Baalen, Andrey Kuzmin, Markus Nagel, Peter Couperus, Cedric Bastoul, Eric Mahurin, Tijmen Blankevoort, and Paul Whatmough. Gptvq: The blessing of dimensionality for llm quantization, 2024.

Xiuying Wei, Yunchen Zhang, Xiangguo Zhang, Ruihao Gong, Shanghang Zhang, Qi Zhang, Fengwei Yu, and Xianglong Liu. Outlier suppression: Pushing the limit of low-bit

- transformer language models. *Advances in Neural Information Processing Systems*, 35: 17402–17414, 2022.
- Xiuying Wei, Ruihao Gong, Yuhang Li, Xianglong Liu, and Fengwei Yu. Qdrop: Randomly dropping quantization for extremely low-bit post-training quantization, 2023a.
- Xiuying Wei, Yunchen Zhang, Yuhang Li, Xiangguo Zhang, Ruihao Gong, Jinyang Guo, and Xianglong Liu. Outlier suppression+: Accurate quantization of large language models by equivalent and optimal shifting and scaling. *arXiv preprint arXiv:2304.09145*, 2023b.
- Guangxuan Xiao, Ji Lin, Mickael Seznec, Hao Wu, Julien Demouth, and Song Han. Smoothquant: Accurate and efficient post-training quantization for large language models. In *International Conference on Machine Learning*, pp. 38087–38099. PMLR, 2023.
- Zhewei Yao, Reza Yazdani Aminabadi, Minjia Zhang, Xiaoxia Wu, Conglong Li, and Yuxiong He. Zeroquant: Efficient and affordable post-training quantization for large-scale transformers. *Advances in Neural Information Processing Systems*, 35:27168–27183, 2022.
- Rowan Zellers, Ari Holtzman, Yonatan Bisk, Ali Farhadi, and Yejin Choi. Hellaswag: Can a machine really finish your sentence? In *Proceedings of the 57th Annual Meeting of the Association for Computational Linguistics*, 2019.
- Aohan Zeng, Xiao Liu, Zhengxiao Du, Zihan Wang, Hanyu Lai, Ming Ding, Zhuoyi Yang, Yifan Xu, Wendi Zheng, Xiao Xia, Weng Lam Tam, Zixuan Ma, Yufei Xue, Jidong Zhai, Wenguang Chen, Zhiyuan Liu, Peng Zhang, Yuxiao Dong, and Jie Tang. GLM-130b: An open bilingual pre-trained model. In *The Eleventh International Conference on Learning Representations (ICLR)*, 2023. URL <https://openreview.net/forum?id=-Aw0rrrPUF>.
- Luoming Zhang, Wen Fei, Weijia Wu, Yefei He, Zhenyu Lou, and Hong Zhou. Dual grained quantization: Efficient fine-grained quantization for llm, 2023.

A Appendix

A.1 Quantization Granularity & More Experiment Settings

We first illustrate more quantization preliminaries in [subsubsection A.1.1](#) for users to understand our subsequent content more clearly. Then we benchmark naive PTQ without algorithms in [subsubsection A.1.2](#) to evaluate quantization granularity, and then we can obtain our basic quantization settings based on that in [subsubsection A.1.3](#).

A.1.1 More Preliminaries of quantization

Naive PTQ can be split into four dimensions: bit-width, symmetric/asymmetric, group size, and dynamic/static. 1) *Bit-width*: In this paper, we mainly focus on w4a4, w4a8, w8a8 weight activation quantization, and w2a16, w4a16 weight-only quantization, and other bit-width settings only use to validate our analyses. Since more extreme low-bit quantization can result in unacceptable accuracy loss, whereas settings like w3a16, and w6a6 cannot continuously pack quantized values, our focus is hardware-friendly which can simultaneously improve inference efficiency ²; 2) *Symmetric or asymmetric*: For asymmetric quantization, a zero-point value z will usually be introduced to represent the floating-point zero. Otherwise, the symmetric quantization does not have that adjustable z to adapt various ranges; 3) *Group size*: [Shen et al. \(2020\)](#) first proposes group-wise quantization, which divides each channel of a weight ³ into different groups and employs a different set of scale and zero-point for each group $W_{i,j:j+g}$ with group size g . However, per-tensor ($W_{:,j}$) quantization or per-channel ($W_{i,:}$) quantization can be also seen as group-wise quantization with a larger group size; 4) *Dynamic or static*: Due to variance in activation range for LLM, [Yao et al. \(2022\)](#) first introduces token-wise ($X_{i,:}$) quantization for activation, which dynamically calculates the min/max range for each token during model inference. We also measure dynamic/static per-tensor activation quantization to make a comprehensive comparison.

A.1.2 Quantization Granularity Exploration

Weight-only. For weight-only quantization, the experiments are conducted as described in [Figure 4](#). Drawing from findings from these experiments, we obtain the following conclusions:

- For lower-bit quantization, the precision advantage of asymmetric over symmetric quantization becomes significantly more pronounced.
- Common group sizes, *e.g.*, 64 and 128, are not sensitive to higher-bit quantization. Moreover, the accuracy drop from channel-wise quantization compared to group-wise quantization is non-negligible across model sizes.
- Larger models exhibit better robustness to quantization, with reduced likelihood of numerical overflow at lower bits.

Weight-activation. Since weight-activation quantization can use integer matrix multiplication to speed up inference, per-group quantization for weight, which would slow down the speed of this multiplication, is always ignored in this manner. Therefore, we force per-channel weight quantization in all experiments. As presented in [Figure 5](#), we have arrived at the following conclusions:

- Per-token quantization significantly outperforms static/dynamic per-tensor quantization.

²Weight-only quantization accelerates by reducing memory data volume, and “wxax” quantization further speeds up with low-bit multiplications. w4a8 leverages 8-bit matrix multiplication for acceleration, as detailed in ([Zhang et al., 2023](#)).

³We denote weight $W \in \mathbb{R}^{out \times in}$. The first/second dimension of W represents output/input channels. Notably, we ignore the batch size dimension for activation $X \in \mathbb{R}^{n \times d}$, where n means token number, d means hidden size.

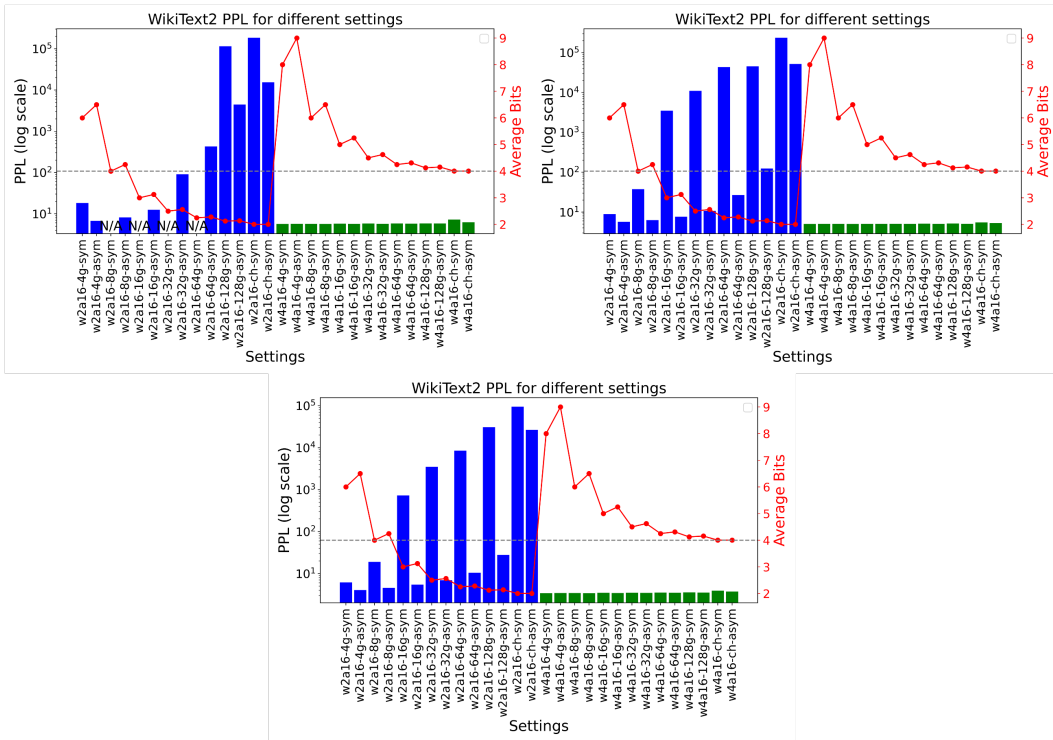


Figure 4: Weight-only quantization granularity results for LLaMA-2-7B (Upper Left), LLaMA-2-13B (Upper Right), and LLaMA-2-70B (Lower Center). asym/sym means asymmetric/symmetric quantization. “ch” means per-channel quantization. “xg” means per-group quantization with group size “x”.

Model	#Bits	PPL ↓			Accuracy (%) ↑					
		WikiText2	C4	Avg.	MMLU	ARC-e	BoolQ	HellaSwag	PIQA	Avg.
LLaMA-2-7B	Full Prec.	5.47	7.26	32.89	46.55	58.38	74.86	73.91	77.69	66.28
	w4a16g128	5.73	7.59	47.10	45.06	56.79	77.40	72.48	77.26	65.79
	w8a8	5.55	33.63	7.35	46.41	57.32	68.96	72.78	77.04	64.50
LLaMA-2-13B	Full Prec.	4.88	6.73	48.82	55.82	75.13	82.39	77.32	79.92	74.12
	w4a16g128	4.98	6.87	52.34	54.43	71.25	81.71	76.37	78.89	72.53
	w8a8	4.92	50.38	6.76	49.77	71.96	74.13	76.96	79.33	70.43
LLaMA-2-70B	Full Prec.	3.32	5.71	20.78	69.52	89.59	87.58	82.12	81.77	82.12
	w4a16g128	3.46	5.83	20.67	68.36	90.30	86.82	81.50	80.85	81.57
	w8a8	3.39	22.17	5.76	61.76	90.12	81.65	81.95	81.39	79.37

Table 8: Ablation results of LLaMA-2 family naive quantization (w4a16g128, w8a8).

Beyond the aforementioned details, we elaborate on the specific size of the downstream data subsets, marked with “*” in the ablation study, used in our paper for ablation studies. We randomly extract 600 questions from MMLU (Hendrycks et al., 2021), 200 from ARC-e (Clark et al., 2018), 300 from BoolQ (Clark et al., 2019), 250 from HellaSwag (Zellers et al., 2019) and 200 from PIQA (Bisk et al., 2020), which can also reflect real model performance.

A.2 More Ablation Study of the Decomposed Algorithm Techniques

In this section, we provide a comprehensive ablation study for different quantization algorithms. We first benchmark weight-only quantization experiments on upstream and subsets of downstream datasets. Based on this research, we find that the trend of PPL across different algorithms and models closely overlaps that of accuracy on the subsets of downstream datasets. Therefore, we only measure PPL for weight-activation quantization exploration along with some conclusions coming from the former weight-only quantization study. On the other hand, we have found that some high-bit (w4a16g128, w8a8) quantization may not be suitable to conduct the ablation study, since their PPL and accuracy are both highly similar to the full-precision models as shown in Table 8. Moreover, we even believe that such relatively high-bit quantization may not require the adoption of any specific algorithm for practical deployment and inference.

Weight-only. As results shown in Table 9, Table 10, Table 11, we make the following conclusions:

- Search-based transformation, especially TS-v1, in weight-only quantization outperforms others. Learning-based transformation employing rule-based transformation, is not a good choice, as the starting point for learning can not gain a good performance.
- Asymmetric clipping helps prevent accuracy drops more than symmetric clipping, especially at lower-bit.
- We obtain our two best practices for weight-only quantization. 1) *TS-v1+CS-asym*: An efficient strategy without learning, and outperforms learning-based methods. 1) *TSv1+CL w/ CS-asym init.*: Take more time (Learn clipping bounds from CS-asym initialization.), but may have higher performance. However, the result of the first best practice in some 3-bit quantization cases, e.g., w3a16g128 LLaMA-2-70B in Table 11, w3a16g128 LLaMA-2-13B in Table 10, offers higher accuracy than the latter.

Weight-activation. We directly apply CS-asym from the conclusion in weight-only study. When quantizing activations, learning-based transformation can help a lot (Shao et al., 2023). Therefore, we explore the different start points for learning, and all of our conclusions from Table 12, Table 13, and Table 14, can be exhibited as follows:

#Bits	Method	PPL ↓			Accuracy (%) ↑					
		WikiText2	C4	Avg.	MMLU*	ARC-e*	BoolQ*	HellaSwag*	PIQA*	Avg.
Full Prec.	-	5.47	7.26	6.37	46.82	62.31	76.33	72.40	79.00	67.37
	TR	6.69	9.11	7.90	41.03	47.24	73.00	68.00	78.50	61.55
	TS-v1	6.46	8.59	7.53	38.20	53.77	69.33	66.80	76.00	60.82
	TS-v2	6.60	8.88	7.74	39.84	45.23	65.67	68.80	77.00	59.31
	TL	6.42	8.62	7.52	39.13	49.25	71.00	67.60	77.00	60.80
	CM	6.66	8.98	7.82	39.42	44.22	68.00	68.00	79.00	59.73
	CS-sym	6.28	8.38	7.33	44.22	41.21	76.67	68.00	77.00	61.42
	CS-asym	6.22	8.32	7.27	41.87	43.22	73.67	69.60	77.00	61.07
	CL	6.21	8.32	7.27	44.86	52.26	71.33	69.20	77.00	62.93
	RH	6.33	8.53	7.43	41.48	50.75	72.00	69.60	77.50	62.27
	TS-v1+RH	6.31	8.51	7.41	38.69	51.26	69.67	69.60	78.00	61.44
	TS-v1+CS-sym	6.22	8.28	7.25	22.83	24.62	58.33	22.40	55.50	36.74
	TS-v1+CS-asym	6.18	8.24	7.21	28.86	24.62	65.67	59.60	68.00	49.33
	TS+CL w/ CS-asym init.	5.94	8.10	7.02	42.26	47.74	74.00	70.40	79.50	62.78
w3a16g128	TR	178.47	119.11	148.79	23.70	27.64	46.67	40.00	58.00	39.20
	TS-v1	34.68	34.47	34.58	24.11	29.15	58.33	44.40	56.00	42.40
	TS-v2	95.22	82.29	88.76	23.04	31.66	43.00	42.40	61.50	40.32
	TL	39.94	47.66	43.80	25.28	29.65	50.33	44.00	58.50	41.55
	CM	421.33	559.34	490.34	NaN	30.15	42.67	41.20	60.50	NaN
	CS-sym	2.18e5	1.65e5	1.91e5	22.83	24.12	58.33	25.60	55.50	37.28
	CS-asym	13.61	18.97	16.29	28.18	22.61	59.67	56.40	68.00	46.97
	CL	11.55	13.96	12.76	27.81	28.64	60.67	55.60	69.50	48.44
	RH	15.85	19.90	17.88	28.70	28.14	53.33	51.60	68.00	45.96
	TS-v1+RH	15.75	19.77	17.76	26.72	31.66	53.00	50.00	60.50	44.38
	TS-v1+CS-sym	2.09e5	1.59e5	1.84e5	22.83	24.62	58.33	22.40	55.50	36.74
	TS-v1+CS-asym	11.69	14.83	13.26	28.86	24.62	65.67	59.60	68.00	49.33
	TS-v1+CL w/ CS-asym init.	8.66	12.30	10.48	31.79	31.16	64.67	57.60	69.50	50.94

Table 9: Ablation results of LLaMA-2-7B weight-only quantization. * means the subset of the corresponding dataset.

#Bits	Method	PPL ↓			Accuracy (%) ↑					
		WikiText2	C4	Avg.	MMLU*	ARC-e*	BoolQ*	HellaSwag*	PIQA*	Avg.
w3a16g128	Full Prec.	4.88	6.73	5.81	56.69	74.37	82.33	75.60	81.00	74.00
	TR	5.56	7.63	6.60	49.84	63.82	78.67	72.00	79.00	68.67
	TS-v1	5.43	7.42	6.42	56.11	65.83	77.00	74.00	79.50	70.49
	TS-v2	5.47	7.51	6.49	50.63	65.33	76.33	73.20	76.50	68.40
	TL	5.44	7.48	6.46	52.36	65.33	73.67	73.60	78.50	68.69
	CM	5.52	7.58	6.55	50.48	64.32	78.00	74.00	77.50	68.86
	CS-sym	5.36	7.37	6.37	53.29	70.35	78.67	72.00	78.00	70.46
	CS-asym	5.35	7.34	6.34	54.40	70.35	80.33	74.00	80.50	71.92
	CL	5.42	7.40	6.41	52.48	59.80	75.00	74.80	77.50	67.92
	RH	5.55	7.67	6.61	53.34	69.85	77.67	73.20	79.00	70.61
	TS-v1+RH	5.41	7.45	6.43	53.37	61.31	76.33	74.00	78.00	68.60
	TS-v1+CS-sym	5.32	7.30	6.31	55.56	67.84	79.33	75.20	80.00	71.59
	TS-v1+CS-asym	5.30	7.28	6.29	55.33	72.36	81.00	74.40	80.50	72.72
	TS-v1+CL w/ CS-asym init.	5.23	7.28	6.26	53.95	70.85	79.00	74.00	80.50	71.66
w2a16g64	TR	16.39	19.39	17.89	25.83	34.17	57.67	54.80	61.00	46.69
	TS-v1	12.30	15.45	13.88	26.63	34.67	55.00	58.80	70.00	49.02
	TS-V2	14.36	17.05	15.71	25.50	32.66	43.33	53.20	64.50	43.84
	TL	12.39	15.76	14.08	26.24	33.67	52.33	55.20	69.00	47.29
	CM	26.22	30.46	28.43	23.89	31.66	51.00	36.40	53.00	39.19
	CS-sym	1.25e5	9.73e4	1.11e5	28.10	17.09	58.33	26.00	47.00	35.30
	CS-asym	8.96	12.52	10.74	32.65	33.67	63.00	60.40	72.00	52.34
	CL	8.40	11.02	9.71	32.45	34.67	64.00	64.00	71.50	53.32
	RH	9.51	12.61	11.06	31.77	31.16	66.00	60.00	73.00	52.39
	TS-v1+RH	9.81	12.99	11.40	35.01	31.66	60.00	56.80	70.50	50.79
	TS-v1+CS-sym	1.22e5	1.22e5	1.22e5	28.10	17.09	58.33	26.00	47.00	35.30
	TS-v1+CS-asym	7.88	10.84	9.36	39.57	43.72	71.00	64.40	74.50	58.64
	TS-v1+CL w/ CS-asym init.	6.97	10.01	8.49	41.53	42.21	67.67	68.80	76.50	59.34

Table 10: Ablation results of LLaMA-2-13B weight-only quantization. * means the subset of the corresponding dataset.

Method	PPL ↓			Accuracy (%) ↑					
	WikiText2	C4	Avg.	MMLU*	ARC-e*	BoolQ*	HellaSwag*	PIQA*	Avg.
Full Prec.	3.32	5.71	4.52	70.91	88.44	83.33	80.00	83.50	81.24
TR	3.95	6.24	5.10	65.40	86.93	82.00	80.40	82.50	79.45
TS-v1	3.85	6.12	4.99	68.14	88.44	83.00	79.20	83.00	80.36
TS-v2	3.93	6.21	5.07	66.62	87.94	82.33	79.20	83.50	79.92
CM	3.98	6.27	5.13	64.90	88.94	79.33	78.00	83.00	78.83
CS-sym	3.85	6.13	4.99	66.34	89.95	82.00	79.20	83.00	80.10
CS-asym	3.84	6.14	4.99	66.03	91.46	83.00	79.20	82.50	80.44
CL	3.81	6.09	4.95	68.90	86.93	81.00	80.00	84.00	80.17
RH	3.93	6.17	5.05	68.01	87.94	84.00	79.20	82.00	80.23
TS-v1+RH	3.95	6.18	5.07	65.66	86.93	83.67	79.20	81.50	79.39
TS-v1+CS-sym	3.75	6.05	4.90	68.38	85.93	83.67	82.40	84.00	80.88
TS-v1+CS-asym	3.74	6.04	4.89	68.21	89.45	84.00	81.60	82.50	81.15
TS-v1+CL w/ CS-asym init.	3.74	6.04	4.89	68.86	88.44	85.00	80.00	81.00	80.66

Table 11: Ablation results of LLaMA-2-70B weight-only (w3a16g128) quantization. * means the subset of the corresponding dataset.

- We still find that TS-v1 has fewer accuracy drops than other learning-free transformation methods. In w4a4 experiments at Table 12, we try different start points for TL and notice that TS-v1 can help gain satisfactory model precision.
- We also provide two best practices aligned with weight-only quantization, *e.g.*, 1) *TS-v1+CS-asym*: and 2) *TL w/ TS-v1 init.+CL w/CS-asym init.*.

#Bits	Method	PPL ↓		
		WikiText2	C4	Avg.
Full Prec.	-	5.47	7.26	6.37
w6a6	CM	6.08	8.07	7.07
	TR	6.29	8.08	7.18
	TS-v1	5.86	7.71	6.79
	TS-v2	5.84	7.76	6.80
	TL+CL	5.97	8.21	7.09
	TS-v1+CS-asym	5.78	7.72	6.75
	TL w/ TS-v1 init. +CL w/ CS-asym init.	5.77	7.68	6.72
w4a8	CM	6.19	8.29	7.24
	TR	6.41	8.56	7.49
	TS-v1	6.22	8.18	7.16
	TS-v2	6.29	8.35	7.32
	TL+CL	5.97	7.93	6.95
	TS-v1+CS-asym	5.89	7.78	6.83
	TL w/ TS-v1 init. +CL w/ CS-asym init.	5.85	7.74	6.80
w4a4	CM	409.53	433.34	421.44
	TR	51.21	61.52	56.37
	TS-v1	15.43	20.01	17.72
	TS-v2	49.41	104.95	77.18
	TL w/ TR init.	17.11	21.09	19.10
	TL w/ ones init.	37.13	45.94	41.54
	TL w/ TS-v1 init.	15.41	19.80	17.61
	TL+CL	13.79	19.12	16.46
	TS-v1+CS-asym	15.66	21.67	18.67
	TL w/ TS-v1 init.+CL w/ CS-asym init.	13.32	18.65	15.99

Table 12: Ablation results of LLaMA-2-7B weight-activation quantization. Ones init. means we set all of elements in s as one before learning.

In a word, we have found four best practices, two for weight-only quantization, and the other two for weight-activation quantization. Furthermore, we suggest that users use the learning-free best practices for relatively higher-bit quantization and learning-based best practices for others.

A.3 More Experiments Validating the Effectiveness of Best Practice

In this section, we present additional experimental results to further validate the effectiveness of our proposed best practices for model quantization. Specifically, we focus on weight-only and weight-activation quantization for the LLaMA-2 model across various sizes (7B, 13B, and 70B). The following tables summarize the main results of these experiments, demonstrating the effectiveness of our best practices in mitigating the impact of quantization on model performance across different configurations (Table 15, Table 16, Table 17, Table 18, Table 19, Table 20).

Weight-only. Our weight-only quantization experiments, as shown in Table 15, Table 16, and Table 17, provide compelling evidence that our best practices significantly preserve model performance, even under low bit settings. Notably, our methodologies achieve SOTA performance. For instance, in the w3a16 setting, the 7B model (Table 15) maintains an

#Bits	Method	PPL ↓		
		WikiText2	C4	Avg.
Full Prec.	-	4.88	6.73	5.81
w6a6	CM	5.32	7.22	6.27
	TR	5.16	7.07	6.12
	TS-v1	5.12	7.02	6.07
	TS-v2	5.13	7.03	6.08
	TL+CL	5.11	7.02	6.07
	TS-v1+CS-asym	5.11	7.00	6.06
	TL w/ TS-v1+CL w/ CS-asym init.	5.07	6.97	6.02
w4a8	CM	5.24	7.19	6.22
	TR	6.41	8.56	7.49
	TS-v1	5.22	7.14	6.18
	TS-v2	5.24	7.17	6.21
	TL+CL	5.78	7.88	6.83
	TS-v1+CS-asym	5.09	6.99	6.04
	TL w/ TS-v1+CL w/ CS-asym init.	5.06	6.97	6.02
w4a4	CM	598.97	687.75	643.36
	TR	22.86	30.50	26.68
	TS-v1	16.59	18.96	17.78
	TS-v2	36.70	55.86	46.28
	TL+CL	12.27	18.38	15.32
	TS-v1+CS-asym	15.29	20.96	18.13
	TL w/ TS-v1 init. +CL w/ CS-asym init.	10.24	13.75	12.01

Table 13: Ablation results of LLaMA-2-13B weight-activation quantization.

#Bits	Method	PPL ↓		
		WikiText2	C4	Avg.
Full Prec.	-	3.32	5.71	4.52
w6a6	CM	4.67	7.62	6.15
	TR	3.66	6.06	4.86
	TS-v1	3.63	6.04	4.84
	TS-v2	3.64	6.04	4.84
	TL+CL	3.73	6.13	4.93
	TS-v1+CS-asym	3.65	6.05	4.85
	TL w/ TS-v1 init. +CL w/ CS-asym init.	3.63	6.02	4.82
w4a8	CM	3.76	6.07	4.91
	TR	3.81	6.14	4.98
	TS-v1	3.68	5.99	4.84
	TS-v2	3.72	6.04	4.88
	TL+CL	7.73	11.30	9.52
	TS-v1+CS-asym	3.53	5.89	4.71
	TL w/ TS-v1 init. +CL w/ CS-asym init.	3.57	5.92	4.75
w4a4	CM	NaN	NaN	NaN
	TR	22.37	37.10	29.74
	TS-v1	15.10	21.48	18.29
	TS-v2	58.32	72.73	65.53
	TL+CL	308.03	241.52	274.78
	TS-v1+CS-asym	14.22	20.27	17.24
	TL w/ TS-v1 init. +CL w/ CS-asym init.	14.22	20.27	17.24

Table 14: Ablation results of LLaMA-2-70B weight-activation quantization.

average accuracy decrement of only 4.13% compared to the full-precision model. Similarly, the 13B model (Table 16) exhibits an average accuracy reduction of 2.6%. Intriguingly, the 70B model (Table 17) demonstrates the most striking resilience with a mere average accuracy decline of 0.07%, suggesting that our best practices are particularly effective at scale.

These results indicate the robustness of our quantization strategies and underscore the potential for their application in larger, more complex models. By enabling more efficient deployment without substantial loss in performance, our best practices for weight-only quantization facilitate wider accessibility and applicability of large-scale language models.

Weight-activation. Advancing from weight-only to weight-activation quantization, our experiments (Table 18, Table 19, and Table 20) provide a more nuanced understanding of quantization effects. This analysis involved subjecting both the weights and activations of the LLaMA-2 model to quantization.

A comparative analysis of the results shows that weight-activation quantization, while generally inducing a higher performance drop compared to weight-only quantization, can still maintain commendable model accuracy when employing our best practices. For instance, in the w6a6 setting, the degradation in model accuracy for the 7B model under weight-activation quantization (Table 18) was contained to an average of 7.07% below full precision. For the 13B model (Table 19), the average performance diminution was somewhat restrained to 10.87%, and the 70B model (Table 20) showed a decline of 10.98%.

#Bits	Method	Accuracy (%) \uparrow					
		MMLU	ARC-e	BoolQ	HellaSwag	PIQA	Avg.
Full Prec.	-	46.51	58.20	74.98	73.95	77.75	66.28
w3a16g128	Naive	38.42	44.09	68.32	70.49	75.73	59.41
	GPTQ	43.43	47.44	72.42	71.01	76.22	62.10
	AWQ	39.94	49.56	72.78	70.86	76.61	61.95
	OmniQuant	42.22	48.15	71.41	70.22	76.06	61.61
	TS-v1+CS-asym	42.33	47.09	71.44	70.93	76.17	61.59
	TS-v1+CL w/ CS-asym init.	41.83	47.62	73.55	70.6	77.15	62.15
w2a16g64	Naive	NaN	26.98	45.93	38.44	58.54	NaN
	GPTQ	25.85	28.22	55.38	51.45	67.30	45.64
	AWQ	25.38	24.87	62.17	24.83	51.20	37.69
	OmniQuant	27.04	29.10	63.88	53.97	69.48	48.69
	TS-v1+CS-asym	27.40	25.40	63.27	57.40	70.40	48.77
	TS-v1+CL w/ CS-asym init.	31.02	31.04	68.17	57.72	71.06	51.80

Table 15: Main results of LLaMA-2-7B weight-only quantization.

A.4 KV Cache Quantization

This part shows the accuracy of KV cache quantization for code generation tasks. From Table 21, we can find that the int8 and int4 KV cache quantization brings almost no accuracy degradation for both the Human-Eval and MBPP dataset. This conclusion is consistent with the case of long context text in the main text, further proving that 4-bit KV cache can be adopted without harm to performance. However, 2-bit KV cache will bring a crash for the generation, and thus should not be adopted.

A.5 Inference Speed

Figure 6 and Figure 7 supplementarily illustrated the speedup brought by various quantization schemes on 1K and 4K input context length. We can find that the conclusion is the same as the 32K input context length in the main text. The w8a8 setting significantly improves the prefill speed and the weight-only quantization helps the decoding speed. The int8 KV cache quantization does not affect the speed much but helps a lot for reducing memory

#Bits	Method	Accuracy (%) \uparrow					
		MMLU	ARC-e	BoolQ	HellaSwag	PIQA	Avg.
Full Prec.	-	55.49	75.13	82.42	77.31	79.92	74.05
w3a16g128	Naive	50.82	65.26	77.40	74.53	78.18	69.24
	GPTQ	53.09	70.19	79.20	74.71	79.33	71.30
	AWQ	52.13	68.43	80.64	74.99	78.29	70.90
	OmniQuant	50.16	63.32	78.38	74.62	78.62	69.02
	TS-v1+CS-asym	51.41	72.84	80.34	75.09	78.62	71.66
	TS-v1+CL w/ CS-asym init.	52.09	70.37	79.94	74.68	79.11	71.24
w2a16g64	Naive	25.76	27.87	56.30	33.32	56.09	39.87
	GPTQ	32.57	32.28	64.92	59.88	70.62	52.05
	AWQ	27.04	20.81	62.17	24.09	52.12	37.25
	OmniQuant	30.00	31.57	70.95	62.81	71.82	53.43
	TS-v1+CS-asym	36.88	47.09	67.83	65.16	74.37	58.27
	TS-v1+CL w/ CS-asym init.	40.58	44.8	71.10	65.29	74.65	59.28

Table 16: Main results of LLaMA-2-13B weight-only quantization.

Method	Accuracy (%) \uparrow					
	MMLU	ARC-e	BoolQ	HellaSwag	PIQA	Avg.
Full Prec.	70.91	88.44	83.33	80.00	83.50	81.24
Naive	65.27	87.83	83.94	79.33	80.58	79.39
GPTQ	67.52	88.18	85.11	80.28	80.63	80.34
AWQ	67.54	87.65	86.57	81.11	81.88	80.95
OmniQuant	67.24	88.36	84.74	80.88	81.77	80.60
TS-v1+CS-asym	67.07	89.95	86.30	80.95	81.07	81.07
TS-v1+CL w/ CS-asym init.	67.78	89.42	87.09	80.91	81.18	81.28

Table 17: Main results of LLaMA-2-70B (w3a16g128) weight-only quantization.

consumption for long context length. Figure 8 shows the speed up on the Drive Orin edge GPU. It can be seen that weight-only quantization also helps the prefill under this setting, which is different from cloud GPUs.

A.6 Mix-precision Quantization

In this section, we present detailed analyses for mix-precision quantization, which can be concisely classified into magnitude-based (Ashkboos et al., 2023; Dettmers et al., 2022; Kim et al., 2024) and Hessian-based (Dettmers et al., 2023; Lee et al., 2023) mix-precision in LLM quantization. In weight-only quantization, previous methods mainly consider the latter type, since Hessian information can help capture weight sensitivity towards quantization. In weight-activation quantization, recent studies only utilize the former type, due to it is efficient to allocate bits to a model. Moreover, the Taylor expansion underlying Hessian information may not be suitable for approximating the impact of quantization, when weight and activation are being quantized with relatively extensive quantization error rather than weight-only quantization.

- **Weight-only.** As shown in Table 22, we have found that utilizing Hessian Disturb. (Dettmers et al., 2023) as the bit allocation metric outperforms Hessian Diag. (Lee et al., 2023) in all configurations. Notably, in order to keep a fair comparison, we employ naive quantization as a baseline, the same as the following weight-activation experiments. Moreover, we have to maintain their bit allocation granularities in the same setting. We choose column-wise mix-precision, due to it can help gain speedup during the hardware inference. Based on that conclusion,

#Bits	Method	Accuracy(%) ↑					
		MMLU	ARC-e	BoolQ	HellaSwag	PIQA	Avg.
Full Prec.	-	46.55	58.38	74.86	73.91	77.69	66.28
w6a6	Naive	42.30	36.16	58.9	71.00	75.84	56.84
	SmoothQuant	45.66	41.09	58.93	71.96	77.04	58.94
	OS+	44.11	42.50	60.24	71.80	76.39	59.01
	OmniQuant	44.08	38.45	61.28	72.77	77.31	58.78
	TS-v1+CS-asym	45.60	41.27	60.49	72.24	77.20	59.36
	TL w/ TS-v1+CL w/ CS-asym init.	45.26	42.5	59.76	71.84	76.71	59.21
w4a8	Naive	40.00	46.74	62.32	71.23	75.79	59.22
	SmoothQuant	41.02	40.56	61.90	70.58	76.17	58.05
	OS+	40.29	46.38	61.38	70.46	75.35	58.77
	OmniQuant	44.24	41.09	68.84	71.22	76.39	60.36
	TS-v1+CS-asym	45.36	50.09	68.26	71.91	76.71	62.47
	TL w/ TS-v1+CL w/ CS-asym init.	44.60	44.44	69.11	71.51	76.55	61.24
w4a4	Naive	24.16	24.34	50.7	30.31	54.03	36.71
	SmoothQuant	26.33	25.57	50.52	48.68	58.98	42.02
	OS+	26.04	25.93	51.16	49.28	62.35	42.95
	OmniQuant	25.97	28.04	53.85	54.65	63.06	45.11
	TS-v1+CS-asym	26.84	21.87	50.89	54.43	64.04	43.61
	TL w/ TS-v1+CL w/ CS-asym init.	28.76	23.63	52.54	58.10	67.03	46.01

Table 18: Main results of LLaMA-2-7B weight-activation quantization.

#Bits	Method	Accuracy(%) ↑					
		MMLU	ARC-e	BoolQ	HellaSwag	PIQA	Avg.
Full Prec.	-	55.82	75.13	82.39	77.32	79.92	74.12
w6a6	Naive	34.20	56.26	58.87	75.67	77.91	60.58
	SmoothQuant	36.37	57.50	61.77	75.74	78.07	61.89
	OS+	36.13	61.73	61.77	75.88	78.24	62.75
	OmniQuant	38.25	58.38	62.51	76.24	78.89	62.85
	TS-v1+CS-asym	37.40	60.32	61.47	75.93	78.29	62.68
	TL w/ TS-v1+CL w/ CS-asym init.	37.37	60.67	62.57	76.47	79.16	63.25
w4a8	Naive	45.21	65.08	73.58	75.42	79.00	67.66
	SmoothQuant	41.02	61.38	71.38	73.33	77.37	64.90
	OS+	45.14	66.31	73.06	75.14	79.11	67.75
	OmniQuant	35.56	42.68	64.50	73.52	76.39	58.53
	TS-v1+CS-asym	46.23	67.02	71.65	76.20	78.62	67.94
	TL w/ TS-v1+CL w/ CS-asym init.	47.70	67.9	73.98	75.95	79.27	68.96
w4a4	Naive	25.51	27.69	47.98	25.95	50.44	35.51
	SmoothQuant	24.51	26.46	51.25	42.16	54.13	39.70
	OS+	24.55	25.93	51.07	42.17	57.62	40.27
	OmniQuant	25.51	27.69	51.71	59.59	65.34	45.97
	TS-v1+CS-asym	24.89	25.40	51.04	54.66	59.09	43.02
	TL w/ TS-v1+CL w/ CS-asym init.	25.74	26.81	52.63	60.98	65.72	46.38

Table 19: Main results of LLaMA-2-13B weight-activation quantization.

#Bits	Method	Accuracy(%) ↑					
		MMLU	ARC-e	BoolQ	HellaSwag	PIQA	Avg.
Full Prec.	-	69.52	89.59	87.58	82.12	81.77	82.12
	Naive	34.88	50.97	59.08	78.97	75.73	59.93
	SmoothQuant	43.70	77.07	68.38	81.19	81.12	70.29
w6a6	OS+	45.50	75.13	67.86	80.86	80.25	69.92
	OmniQuant	40.65	64.37	63.76	79.95	77.97	65.34
	TS-v1+CS-asym	45.14	79.19	67.52	80.82	80.63	70.66
	TL w/ TS-v1+CL w/ CS-asym init.	47.05	80.25	66.88	80.93	80.58	71.14
	Naive	45.21	65.08	73.58	75.42	79.00	67.66
	SmoothQuant	58.78	86.95	78.38	79.51	80.52	76.83
w4a8	OS+	60.93	86.24	78.99	80.16	80.63	77.39
	OmniQuant	25.78	35.45	59.08	59.43	74.86	50.92
	TS-v1+CS-asym	61.53	89.42	82.29	81.48	81.72	79.29
	TL w/ TS-v1+CL w/ CS-asym init.	61.10	88.54	79.60	80.42	81.39	78.21
	Naive	NaN	NaN	NaN	NaN	NaN	NaN
	SmoothQuant	24.27	23.1	50.89	57.00	56.69	42.39
w4a4	OS+	25.28	24.87	49.97	45.98	51.47	39.51
	OmniQuant	25.12	25.04	49.36	29.34	53.10	36.39
	TS-v1+CS-asym	25.44	25.04	50.4	47.87	56.75	41.10
	TL w/ TS-v1+CL w/ CS-asym init.	25.26	23.63	51.10	51.34	57.83	41.83

Table 20: Main results of LLaMA-2-70B weight-activation quantization.

Model	KV Cache Prec.	Pass@1 (%) ↑		
		Human-Eval	MBPP	Avg.
LLaMA-2-7B	Full Prec.	12.80	22.00	17.40
	int8	13.41	20.00	16.71
	int4	13.41	21.00	17.21
	int2	0.00	0.00	0.00
	w4a8kv4	12.20	18.40	15.30
LLaMA-2-13B	Full Prec.	18.29	24.00	21.15
	int8	17.68	23.00	20.34
	int4	17.68	23.00	20.34
	int2	0.00	0.00	0.00
	w4a8kv4	15.85	23.40	19.63
LLaMA-2-70B	Full Prec.	29.27	42.00	35.64
	int8	29.88	38.00	33.94
	int4	30.49	39.00	34.75
	int2	0.00	0.00	0.00
	w4a8kv4	29.27	38.20	33.74

Table 21: KV cache quantization results on LLAMA-2 series models.

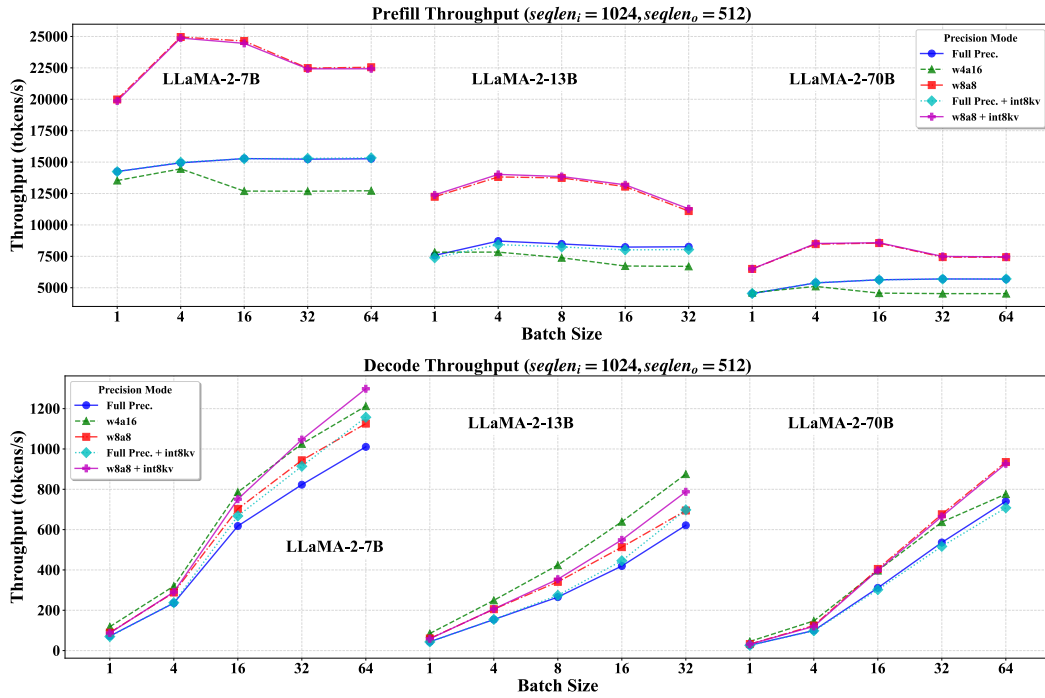


Figure 6: Inference speed of 7B, 13B, and 70B LLaMA-2 models on NVIDIA A100 GPU. (Input sequence length: 1024, Output sequence length: 512)

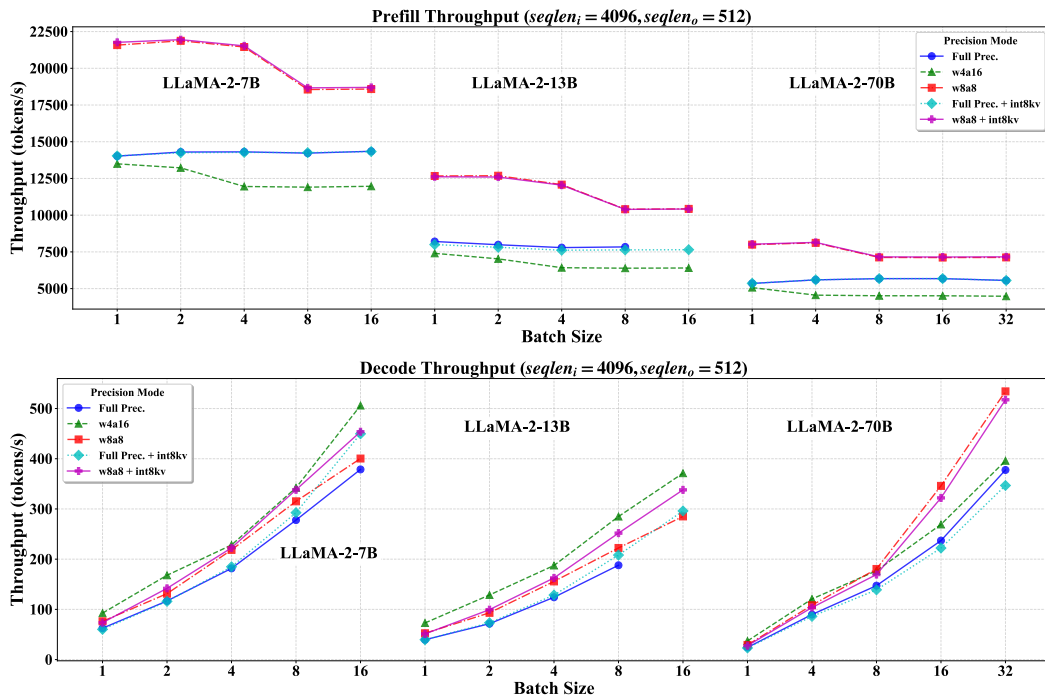


Figure 7: Inference speed of 7B, 13B, and 70B LLaMA-2 models on NVIDIA A100 GPU. (Input sequence length: 4096, Output sequence length: 512)

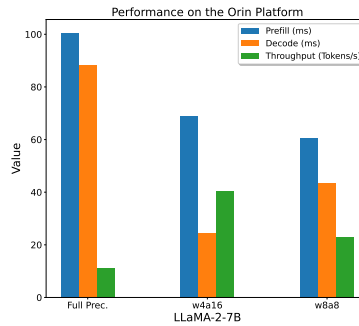


Figure 8: Throughput comparison of quantization on the edge GPU (Drive Orin). (Token/s)

we conducted the mixture rate experiment for Hessian Disturb. column-wise methods in Table 23. We have found that in 3-bit quantization, performance between high (20%) and low (10%) mixture rates are closely similar. However, in 2-bit quantization, a high (20%) mixture rate for an LLM with a relatively small model size (7B) can gain significant accuracy improvement. More experiments for fix-precision algorithms combined with mix-precision strategy are required to be evaluated in the future.

- **Weight-activation.** In Table 24, we measure two kinds of magnitude mix-precision strategies: Dynamic (Dettmers et al., 2022) and Static (Ashkboos et al., 2023). Although the former brings non-negligible inference overhead, it exhibits higher accuracy rather than Static. Considering our design principles, we try to allocate more columns in full-precision in the Static strategy and try to keep Down layers in the LLM in 8-bit, since it is more sensitive to quantization (Heo et al., 2023; Ashkboos et al., 2023). However, all of them are still inferior to the Dynamic method, therefore, it is necessary to explore new algorithms for inference-efficient static weight-activation mix-precision quantization.

Model	#Bits	Metric	Granularity	PPL ↓			
				WikiText2	C4	Avg.	
LLaMA-2-7B	Full Prec.	-	-	5.47	7.26	6.37	
		-	-	6.66	8.98	7.82	
		Hessian Diag.	column	5.99	7.97	6.98	
	w3a16g128	Hessian Disturb.	column	5.92	7.88	6.90	
		Hessian Disturb.	element	5.92	7.85	6.89	
		-	-	421.33	559.34	490.34	
	w2a16g64	Hessian Diag.	column	10.30	13.46	11.88	
		Hessian Disturb.	column	8.91	11.79	10.35	
		Hessian Disturb.	element	8.54	11.54	10.04	
	LLaMA-2-13B	Full Prec.	-	-	4.88	6.73	5.81
			-	-	5.52	7.58	6.55
			Hessian Diag.	column	5.25	7.20	6.22
w3a16g128		Hessian Disturb.	column	5.19	7.13	6.16	
		Hessian Disturb.	element	5.16	7.06	6.11	
		-	-	26.22	30.46	28.43	
w2a16g64		Hessian Diag.	column	7.71	10.51	9.11	
		Hessian Disturb.	column	7.21	9.90	8.55	
		Hessian Disturb.	element	6.65	9.17	7.91	
LLaMA-2-70B		Full Prec.	-	-	3.32	5.71	4.52
			-	-	3.98	6.27	5.13
			Hessian Diag.	column	3.68	5.97	4.83
	w3a16g128	Hessian Disturb.	column	3.63	5.94	4.79	
		Hessian Disturb.	element	3.63	5.94	4.79	
		-	-	10.32	15.16	12.74	
	w2a16g64	Hessian Diag.	column	5.33	7.76	6.54	
		Hessian Disturb.	column	5.05	7.35	6.20	
		Hessian Disturb.	element	4.70	6.97	5.84	

Table 22: Weight-only mixed-precision quantization results (20% mixture rate). Hessian Diag. uses the magnitude of diagonal elements of the Hessian matrix to determine bit allocation to the corresponding column. Hessian Disturb. utilizes the Hessian matrix, approximating the disturbance influence coming from the quantized weights, to determine their quantization bit.

Model	#Bits	Mixture Rate (%)	PPL ↓		
			WikiText2	C4	Avg.
LLaMA-2-7B	Full Prec.	0	5.47	7.26	6.37
		0	6.66	8.98	7.82
		1	6.35	8.54	7.45
	w3a16g128	5	6.13	8.16	7.15
		10	6.06	8.05	7.06
		20	5.92	7.88	6.90
	w2a16g64	0	421.33	559.34	490.34
		1	50.44	NaN	NaN
		5	13.00	16.52	14.76
		10	10.94	14.15	12.55
		20	8.91	11.79	10.35
		LLaMA-2-13B	Full Prec.	0	4.88
0	5.52			7.58	6.55
1	5.38			7.38	6.38
w3a16g128	5		5.30	7.27	6.29
	10		5.26	7.22	6.24
	20		5.19	7.13	6.16
w2a16g64	0		26.22	30.46	28.43
	1		13.21	16.12	14.67
	5		8.76	11.77	10.27
	10		8.09	10.95	9.52
	20		7.21	9.90	8.55
	LLaMA-2-70B		Full Prec.	0	3.32
0		3.98		6.27	5.13
1		3.79		6.07	4.93
w3a16g128		5	3.73	6.02	4.88
		10	3.70	5.99	4.85
		20	3.63	5.94	4.79
w2a16g64		0	10.32	15.16	12.74
		1	6.76	9.56	8.16
		5	5.73	8.25	6.99
		10	5.46	7.91	6.69
		20	5.05	7.35	6.20

Table 23: Mixture rate results for weight-only mixed-precision quantization. We employ Hessian Disturb. metric and column-wise granularity.

Model	#Bits	Method	PPL ↓		
			WikiText2	C4	Avg.
LLaMA-2-7B	Full Prec.	-	5.47	7.26	6.37
	w4a4	-	409.53	433.34	421.44
		Dynamic-256	7.36	10.21	8.79
		Static-256	8.56	11.57	10.13
		Static-256+drown_proj (int8)	8.14	10.92	9.53
		Static-512+drown_proj (int8)	7.52	10.20	8.86
LLaMA-2-13B	Full Prec.	-	4.88	6.73	5.81
	w4a4	-	598.97	687.75	643.36
		Dynamic-256	6.54	9.20	7.87
		Static-256	7.58	10.30	8.94
		Static-256+drown_proj (int8)	7.32	10.03	8.68
		Static-512+drown_proj (int8)	6.87	9.45	8.16
LLaMA-2-70B	Full Prec.	-	3.32	5.71	4.52
	w4a4	-	NaN	NaN	NaN
		Dynamic-256	5.33	8.26	6.80
		Static-256	6.83	9.83	8.33
		Static-256+drown_proj (int8)	6.41	9.20	7.81
		Static-512+drown_proj (int8)	5.85	8.49	7.17

Table 24: Weight-activation mix-precision quantization results. Dynamic/Static-“x” means allocating bit during inference (dynamic)/calibration (static) and selecting “x” columns in full-precision. down_proj (int8) means we keep the weight of the Down layer in FFN modules in 8-bit integer type.